

# Equivalent granular void ratio concept for sand-silt mixtures

M.E. Karim & M.J. Alam

*Bangladesh University of Engineering and Technology, Dhaka 1000, Bangladesh*

**ABSTRACT:** Behaviour of sand-silt mixture under cyclic loading and static loading has been studied. In Cyclic Triaxial Test, specimens were prepared by moist tamping method and in Static Test both moist tamping and air pluviation method were used to prepare the soil specimens. For the sand and the nonplastic silt, the Threshold Fines Content ( $F_{th}$ ) and Limiting Fines Content ( $LFC$ ) were found to be equal at 30%. In moist tamping method, the Cyclic Resistance Ratio ( $CRR$ ) and Static Shear Strength ( $SSS$ ) decreased with increasing nonplastic silt content till  $LFC$ ; later it remained near about constant till the time when the specimen was pure silt at constant relative density. However, in air pluviation method, there was a peak  $SSS$  at 5% silt content; later the value decreased with increasing silt content till  $LFC$ , and thereafter it remained constant till the specimen was pure silt. All specimens prepared by air pluviation method showed higher  $SSS$  than those prepared by moist tamping method except clean sand. The concept of equivalent granular void ratio was found to be more appropriate to explain the behaviour of sand-silt mixtures than that of relative density and global void ratio. In both moist tamping and air pluviation methods, the coefficient of permeability decreased with increasing nonplastic silt content till  $LFC$ ; later it remained near about constant till the specimen was pure silt. This variation of coefficient of permeability with silt content was better explained by variation of effective particle size ( $D_{10}$ ) than relative density and void ratio.

## 1 INTRODUCTION

The behavior of sand and non-plastic silt mixtures under cyclic and static loadings has been discussed broadly in geotechnical literature. Nevertheless the conclusions are still conflicting. A number of studies concluded that the presence of nonplastic silt decreased the liquefaction potential/static strength (Tokimatsu & Yoshimi 1983; Seed et al. 1983; Pitman 1994; Yamamuro & Covert 2001; Belkhatir et al. 2011; Arab & Belkhatir 2012; Belkhatir et al. 2013; Yin et al. 2013), some studies indicated that silt increased the liquefaction potential (Troncoso & Verdugo 1985; Sladen et al. 1985), while some other studies reported that the resistance initially decreased as the silt content increased, thereafter increased as the silt content continues to increase (Chang & Kaufman 1982). On the other hand, Dash & Sitharam (2011b) concluded that increasing the silt content increased resistance till 5% silt content; later the resistance (due to cyclic and static loading) decreased with increasing silt content till Limiting Fines Content ( $LFC$ ); after the  $LFC$  the resistance remained about constant till pure silt. Loose sand or sand-silt mixture under undrained shearing can manifest instability under either monotonic or cyclic loading. An important concept in the interpretation of instability is the instability line,  $IL$  (Chu & Leong 2002; Lo et al. 2008). However, a number of recent publications reported that global void ratio  $e$  (Thevanayagam 2000; Rahman et al. 2008; Rahman et al. 2014) is not a good state variable for sandy soil. Thus, equivalent granular void ratio ( $e^*$ ) instead of global void ratio ( $e$ ) is proposed to resolve this problem. Rahman et al. (2008) reported that the steady state ( $SS$ ) data points of sand with various fines can be described by a single trend curve, which is termed as the Equivalent Granular Steady State Line ( $EG-SSL$ ).

The sand and nonplastic silt were collected from the bank of Padma river at Mawa side of proposed Padma Multipurpose Bridge Project, Munshiganj, Bangladesh. Current velocity of rivers of Bangladesh varies significantly in various seasons. In the Padma Bridge Project area, siltation of pure sand was observed during raining season, while silt is deposited in dry season. Sand-silt mixtures are deposited at the start and end of rainy season. During subsoil investigation of Padma Bridge Project, fine sand, silt and sand-silt mixtures were

found at various depths. That is why it is important to know the behavior of Padma sand-silt mixtures under cyclic and static loading. Here the *EG-SSL* for Padma sand-silt is developed. The *EG-SSL* can be used to predict the failure behavior (flow or non-flow) of Padma sand-silt mixtures for cyclic (earthquake) loading and static loading. In undrained static test, soil specimens (each sand-silt mixtures) have been prepared by two methods, namely moist tamping and air pluviation method. In cyclic test, soil specimens have been prepared by moist tamping method only. Permeability test by falling head method have been conducted to see the effect of silt content on permeability of sand-silt mixture. In this paper, we basically verified other researchers' findings on the topic. We have shown that permeability of sand-silt mixtures also depends on the silt content which is new in this paper.

## 2 EXPERIMENTAL PROGRAM

### 2.1 Tested Material

Sand and silt used in this study were collected from sand bars of Padma River, Mawa, Munshiganj, Bangladesh, near the proposed Padma Bridge site. The collected soil samples were first oven dried and then the grain size analysis was conducted. The shape of the sand and silt has been found to be near about similarly angular. Efforts were made to determine the Plastic Limit (*PL*) of silt; however, the silt sample was found to be non-plastic. Index property of sand and silt, namely, specific gravity, maximum and minimum dry density, liquid limit, plastic limit are presented in Table 1.

Table 1. Index properties of studied soil samples

Soil Type	Sand	Silt
USCS classification symbol	SP	ML
Mean particle diameter $D_{50}$ (mm)	0.2	0.02
Uniformity coefficient ( $C_u$ )	2.22	5.82
Coefficient of gradation ( $C_g$ )	1.16	2.15
Specific gradation ( $G_s$ )	2.69	2.72
Liquid limit (%)	N/A	38
Plastic limit (%)	N/A	N/A
Plasticity index	N/A	NP*

NP = Nonplastic

The vibration table method (*ASTM D4253*) is limited to maximum fines content of 15%, while Proctor Compaction tests do not always produce accurate, repeatable result for clean sand. Therefore, vibration table, standard proctor and modified proctor tests were conducted on each sand-silt mixtures. Lee & Fitton (1968) concluded that the vibration table tests yielded maximum dry densities that were about the same as those produced by the Modified Proctor test. So, Modified Proctor test was used for all sand-silt mixtures to determine the maximum dry density. Minimum dry density was determined by free fall in water method (Head 1984).

### 2.2 Threshold Fines Content and Limiting Fines Content

The void ratio achieved decreases with fines content until a threshold value is reached, but further increase in fines content leads to an increase in void ratio. The first segment represent a 'fines in coarse' packing and the second segment representing a 'coarse in fines' packing. And the changing point ('fines in coarse' to 'coarse in fine') is called Threshold Fines Content ( $F_{th}$ ) (Rahman & Lo 2008). To determine the  $F_{th}$ , Rahman & Lo (2008) proposed the following equation:

$$F_{th} = 40 \left( \frac{1}{1 + e^{\alpha - \beta x}} + \frac{1}{x} \right) \quad (1)$$

Where,  $X = D_{10}/d_{50}$ ,  $\alpha = 0.50$ ,  $\beta = 0.13$ ,  $D_{10}$  and  $d_{50}$  for sand and silt respectively. Using the equation (1), the  $F_{th}$  in this study was found 30%.

As fines are added to a sand, it passes from one phase to the other through a transition point called the Limiting Fines Content (*LFC*). It is the point below which the soil structure is mainly silt contained within a sand matrix, whereas beyond this point there are enough fines and such grains loose contact with each other ( $e_{max}$  for sand) (Dash & Sitharam 2011a). The *LFC* is calculated using the following expression (Hazirbaba 2005):

$$LFC = \frac{W_{fines}}{W_{sand} + W_{fines}} = \frac{G_f e_s}{G_f e_s + G_s (1 + e_f)} \quad (2)$$

Where,  $W_{fines}$  is the weight of fines and  $W_{sand}$  is the weight of sand in a sand–silt mixture. Similarly,  $G_f$ ,  $G_s$ ,  $e_f$  and  $e_s$  stand for specific gravity of silt and sand, maximum index void ratio of silt and sand, respectively. Using Eq. (2), the  $LFC$  for sand-silt mixtures used in this investigation was found to be 30%. Here the value of threshold Fines Content and Limiting Fines Content (as per calculation) is equal ( $F_{th} = LFC = 30\%$ ).

The concept of  $LFC$  is an idealization of a transition zone where the soil fabric changes from a silt-in-sand matrix to a sand-in-silt matrix. This transition zone may be narrow, ~2% on either side of a distinct  $LFC$ , (Rahman et al. 2008) or may be "flat and wide" for Sydney sand (Rahman et al. (2011)), about 7% on either side of a not-so-distinct  $LFC$ .

On the other hand, Thevanayagam (2000) proposed that when the  $FC$  (Fines Content)  $> F_{th}$  the finer grains begin to play a rather important role while the role of coarse grains begin to diminish. The fines may carry the contact and shear forces while the coarser grains may act as reinforcing elements embedded within the finer grain matrix. The effect of coarser grains cannot be completely neglected until they are separated sufficiently apart. This imposed a Limiting Fines Content ( $FLC$ ) (Thevanayagam 2000).

### 2.3 Equivalent Void Ratio Calculation

Relative density is a problematic parameter for sand with fines which might be the main reason of conflicting outcome as discussed above. The equivalent granular void ratio ( $e^*$ ) may be a more consistent parameter (Thevanayagam 2002, Rahman et al. 2008, 2014). So to determine the equivalent void ratio the following equations are used:

For intergranular void ratio,

$$(e_c)_{eq} = \frac{e + (1-b)f_c}{1 - (1-b)f_c} \quad (3)$$

For interfine void ratio,

$$(e_f)_{eq} = \frac{e}{f_c + \frac{1-f_c}{R_d^m}} \quad (4)$$

when  $FC > FLC$ ,

$$(e_f)_{eq} = \frac{e}{f_c} \quad (5)$$

where  $e$  = void ratio,  $b$  = portion of fines that contribute to active intergrain contacts,  $R_d$  = particle size disparity ration ( $D_{10}/d_{50}$ ),  $FC$  = fines content,  $m$  = reinforcement factor.

Rahman et al. (2008) proposed a semi-empirical equation expressed as,

$$b = \left[ 1 - \exp\left(-0.3 \frac{(f_c / f_{thre})}{k}\right) \right] x \left( r \frac{f_c}{f_{thre}} \right)^r \quad (6)$$

$0 < b < 1$

where,  $r = (D_{10} / d_{50})^{-1} = d_{50} / D_{10}$ ,  $k = (1 - r^{0.25})$

The vanayagam (2000) proposed that the  $m$ -value will be in-between 0 and 1 ( $0 < m < 1$ ). A relationship among equivalent void ratio ( $e^*$ ),  $FC$ ,  $b$ -value and  $m$ -value at constant void ratio of 0.76 is shown in Figure 1. According to Figure 1.,  $m=0.4$  seems to be more reliable. Therefore,  $m=0.4$  is used to calculate  $e^*$  in this study.

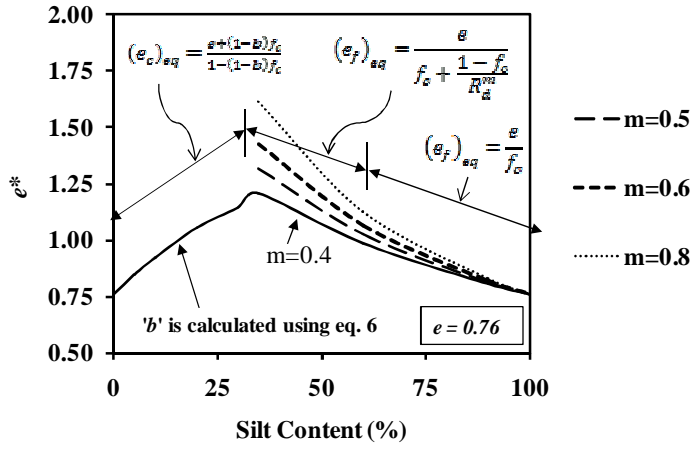


Figure 1. Determination of b and m values

#### 2.4 Sample Preparation, Saturation, Consolidation and Shear

All triaxial tests were carried on 71 mm diameter and 142 mm height specimen. Samples were prepared adding the sand with nonplastic silt of 0 to 100% (percent by dry weight). The specimens were prepared by moist tamping method and air pluvation method. After setting specimen into a triaxial cell, cell pressure was set to 20 kPa and carbon dioxide was passed through the specimen for one hour. Then, distilled water was flowed through the specimen for one hour for sand and three hour for silt. A pressure gauge was fixed with CO<sub>2</sub> cylinder to control CO<sub>2</sub> pressure (at 10 kPa). By measuring the change of cell volume, the void ratio change during CO<sub>2</sub> percolation and distilled water percolation were calculated. In this study, after completion of initial saturation (use of CO<sub>2</sub> and water), back pressure saturation and consolidation at 100 kPa were performed. 1-2 percent change of relative density was noticed after completion of consolidation. The specimen was saturated with sufficient back pressure till the Skempton's B value reached 0.95. The void ratio change during saturation was very minor. So it was neglected. Subsequently the specimen was isotropically consolidated at 100kPa effective confining pressure (for all tests). The duration of consolidation was 1 hour for sand and 3 hours for silt. After consolidation the shearing/cyclic phase started. The cyclic triaxial tests were stress controlled at frequency 1 Hz. The static triaxial tests were undrained strain controlled, at rate of 0.05% axial strain per minute.

#### 2.5 Cyclic Shear Strength and Static Shear Strength

The specimens were loaded with a sinusoidal deviator stress at the appropriate Cyclic Stress Ratio (*CSR*) until the 6% double amplitude axial strain (Karim & Alam 2014) was achieved. It is worth to mention here that 6% double amplitude strain has been used to let the excess pore pressure be develop fully, though it is common to use 5% double amplitude strain. Initial liquefaction (excess pore water pressure becomes equal to the initial effective stress,  $\sigma_{3c}'$ ) or a deformation of 6% double amplitude axial strain at 15th cycle was the criterion used in this study to define the Cyclic Resistance Ratio (*CRR*). A minimum of three cyclic tests were carried out at different Cyclic Stress Ratios to determine *CRR*. Once the *CRR* was determined, the Cyclic Shear Strength (*CSS*) was calculated using Eq. 7 as given below.

$$\sigma_c = 2 \times \sigma_{3c}' \times CRR \quad (7)$$

where,  $\sigma_c$  = Cyclic Shear Strength (kPa),  $\sigma_{3c}'$  = effective confining pressure (kPa), *CRR* = Cyclic Resistance Ratio.

Undrained Static Shear Strength (*SSS*) was determined from the plot of deviator stress verses axial strain. In a particular test the undrained shear stress ( $\tau$ ) of a specimen is the half of deviator stress ( $q = (\sigma_1 - \sigma_3)$ ) (Eq. 8).

$$\tau = q/2 \quad (8)$$

Here the peak deviator stress within 15% axial strain is the deviator strength. *SSS* is the half of deviator strength (*ASTM D4767-11*).

### 3 DISCUSSION

#### 3.1 Cyclic and Static Triaxial Test

The cyclic and static triaxial test results of sand-silt mixtures prepared by moist tamping method are shown in Figure 2; it shows undrained *SSS* and *CSS* as a function of silt content. For both cyclic and static tests, the *CSS* and *SSS* decreased with increasing silt content till *LFC*; thereafter *CSS* and *SSS* became near about constant till the specimen was pure silt. This conclusion matches with that reported by Dash & Sitharam (2011a; 20011b). However, one difference is that Dash & Sitharam (2011a; 2011b) reported peak cyclic and static strength for specimen with 5% silt content, which was not found for specimens prepared by moist tamping method (see Figure 2). It should be noted however that their sample preparation method was air pluviation and the shape of sand was angular and round.

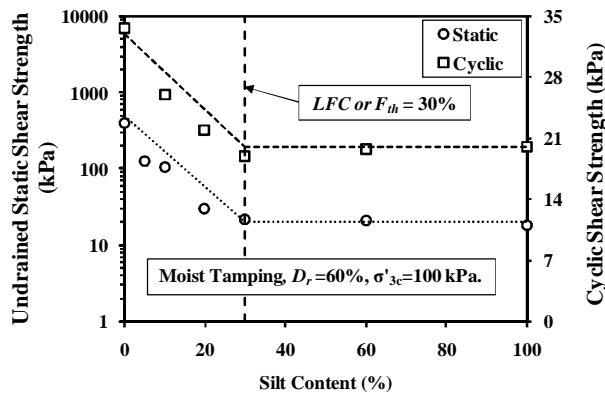


Figure 2. (a) Cyclic and (b) static triaxial test results

#### 3.2 Static Test at Moist Tamping and Air Pluviation Method

Figure 3 shows the effect of nonplastic silt on sand for different sample preparation methods. It shows that in moist tamping method the peak shear stress decreases with increasing silt content till *LFC*; later it becomes near about constant. However, in air pluviation method, there is a peak at 5% silt content. For silt content more than 5% the behaviour is more or less similar to that of moist tamping method. Dash & Sitharam (2011a, b) also reported the same behaviour for air pluviation method. However, we could not find the peak at 5% silt content for specimen prepared with moist tamping method. This means that the behaviour of sand-silt mixture differs depending on the sample preparation method. All specimens prepared by air pluviation method showed higher *SSS* values compared to those obtained for specimens prepared by moist tamping method except clean sand.

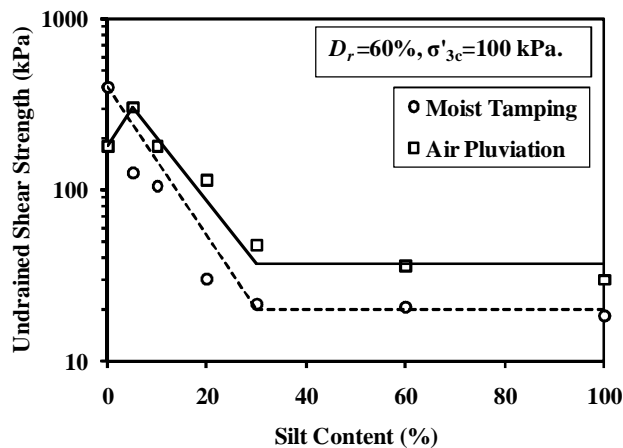


Figure 3. Peak shear stress verses silt content for specimens prepared by moist tamping and air pluviation methods

### 3.3 Implication on Assessment of Liquefaction Potential

Recent studies on liquefaction potential by NCEER working group (Cetin, et al. 2014) showed that based on the overall (regressed) correlation, the energy, procedure, and overburden-corrected  $N$ -values ( $N_{1,60}$ ) are further corrected for fines content as

$$N_{1,60,CS} = N_{1,60} * C_{FINES} \quad (10)$$

where the fines correction ( $C_{FINES}$ ) was “regressed” as a part of the overall Bayesian updating analyses. The fines correction is equal to approximately 1.0 (a null adjustment) for fines contents of  $FC \leq 5\%$ , and reaches a maximum (limiting) value for  $FC \geq 35\%$ . However, findings of current research contradict the correction factor in above equation of assessment of liquefaction potential. According to our findings, before applying this correction factor, one must consider the plasticity index and liquid limit of fines. In case of non plastic fines, increase of fines content decreases the cyclic resistance ratio. Whereas increase of fat clay, lean clay and elastic silt type fines content increases the cyclic resistance ratio. These facts should be considered for further refinement of liquefaction potential analysis.

### 3.4 Permeability Test

The permeability test results of sand-silt mixtures prepared by moist tamping method and air pluviation method are shown in Figure 4. It shows that permeability decreases with increase in nonplastic silt content till LFC; thereafter it is near about constant till the specimen becomes pure silt. This behaviour of decreasing permeability with increasing silt content could not be explained using either the global void ratio or equivalent granular void ratio. Global and equivalent void ratios are indicated in Figure 4. The variation of coefficient of permeability with silt content may be explained by effective particle size ( $D_{10}$ ) variation. Permeability depends on  $D_{10}$  (Hazen 1892, Kresic 1998). The values of  $D_{10}$  for different sand-silt mixtures are shown in Figure 5. It shows that  $D_{10}$  decreases rapidly with increasing silt content of specimen, upto 20% silt content. Above 20% silt content, variation of  $D_{10}$  is not significant. From Figures 4 and 5, it can be seen that decrease of permeability with the increase of silt content can be directly related to change of  $D_{10}$ . From literature it is seen that coefficient of permeability is a function of  $D_{10}^2$ . Therefore, coefficient of permeability has been normalized by dividing it with  $D_{10}^2$  and presented in Figure 6, which clearly shows that  $D_{10}$  is the most important controlling factor for permeability.

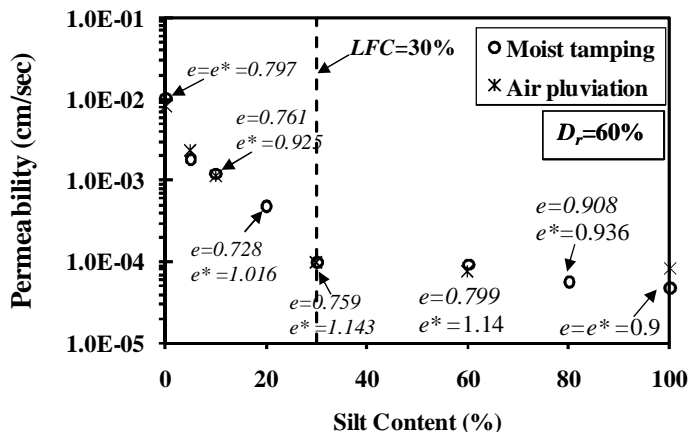


Figure 4. Permeability test results of sand and silt mixtures

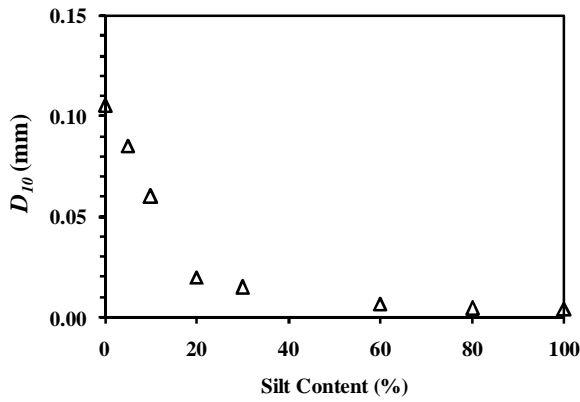


Figure 5.  $D_{10}$  verses silt content.

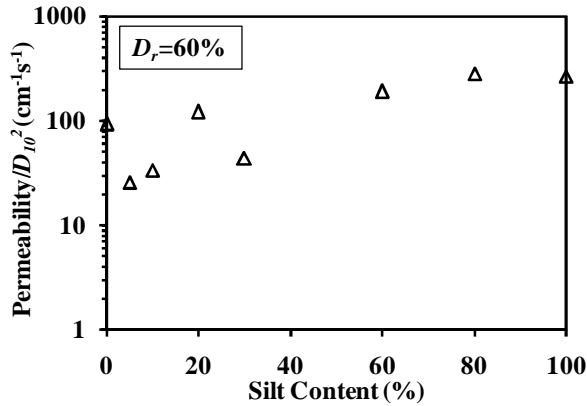


Figure 6. Normalized coefficient of permeability vs. Silt content

### 3.5 Global Void Ratio, Relative Density and Equivalent Granular Void Ratio

The undrained peak shear strength verses silt content at constant global void ratio ( $e$ ) and constant equivalent granular void ratio ( $e^*$ ) are shown in Figure 7. For constant  $e$ , the undrained peak shear strength decrease with increase in silt content till  $F_{th}$  or  $LFC$ ; thereafter it remains near about constant till 60% silt content and again start increasing with increase in silt content till reaching pure silt. This suggests global void ratio is not a good parameter to explain the behaviour of sand-silt mixture. In Figures 2 and 8, it is shown that at constant relative density, static and cyclic shear strength decreases with increasing silt content, which suggests that relative density is not a good parameter to explain the behaviour of sand-silt mixtures. On the other hand, at constant  $e^*$  it is seen that the shear strength of sand silt mixtures remains near about constant. This means that the constant  $e^*$  concept is more appropriate to explain the behaviour of sand-silt mixtures.

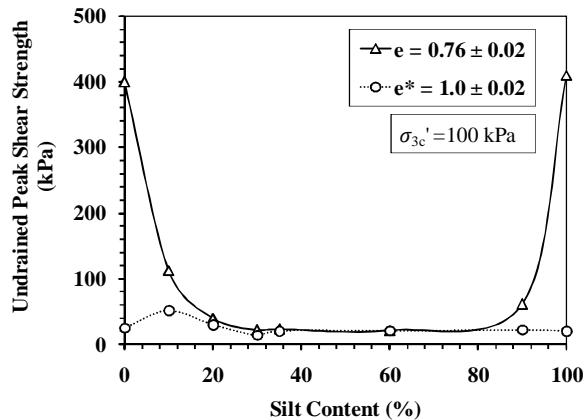
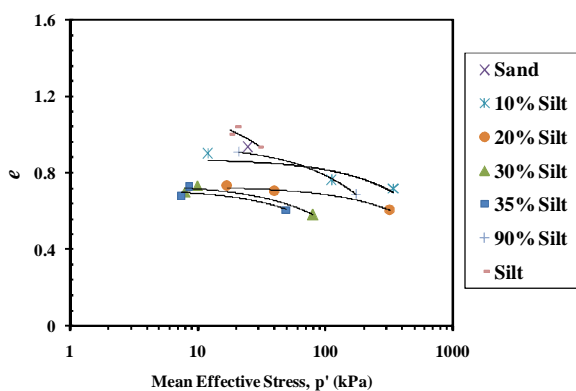


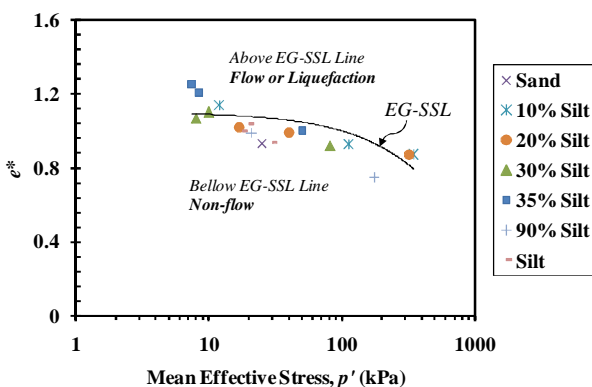
Figure 7. Peak deviator stress verses silt content at constant  $e$  and  $e^*$ .

### 3.6 Equivalent Granular Steady State Line

The  $e - \log(p')$  graph of sand-silt mixtures is shown in Figure 9(a). It shows that the Steady State Line (SSL) of sand-silt mixtures go down ward with increasing in silt content, which was also observed by Murthy et al. (2007). A number of researchers have demonstrated that irrespective of silt, the SS data points in  $e^* - \log(p')$  (see Figure 9(b)) space may be described by a single trend (S. Thevanayagam 2000, Rahman et al. 2014). This single relationship is referred to as “equivalent granular steady state” (*EG-SSL*) (shown in Figure. 20 (b)). Here the *EG-SSL* is independent of fines. The *EG-SSL* obtained from the prediction approach can be used to predict undrained behaviour such as flow, non-flow or limiting flow behaviour under Critical State Soil Mechanics (*CSSM*) framework (Rahman et al. (2010)).  $\psi^*(0) > 0$ , ( $\psi^*$  = Equivalent Granular State Parameter =  $e^* - e_{ss}^*$ ) shows flow-type behaviour;  $\psi^*(0) < 0$ , shows non-flow behaviour; and at  $\psi^*(0) \approx 0$ , shows limited flow behaviour (Rahman et al, 2014). Therefore, equivalent granular steady line concept was found to be valid from the data of this study.



(a)



(b)

Figure 9. (a) Steady State Line (SSL) with increase in fines content and (b) Equivalent Granular Steady State Line (*EG-SSL*) of studied sand and silt.

## 4 CONCLUSIONS

Sand and nonplastic silt were mixed at different proportions (0 to 100% silt). Cyclic triaxial tests were conducted on specimens prepared by moist tamping method. Undrained static tests were conducted on sand-silt mixtures prepared by moist tamping and air pluviation methods. Permeability test by falling head method were also conducted for specimens prepared by both methods. The effects of the silt content on the sand for cyclic and static loadings were examined.

In cyclic loading, after developing 80 percent excess pore water pressure, all specimens become initially unstable. But the specimens with silt content less than *LFC* show split or dilative behaviour.

In moist tamping method, the *CRR* and *SSS* decrease with increasing nonplastic silt content till *LFC*; later it remains near about constant till the specimens become pure silt at constant relative density. However, in air pluviation method there is a peak *SSS* at 5% silt content; beyond that *CRR* and *SSS* decrease with increasing

silt content till *LFC*; thereafter it shows constant behaviour till the specimens become pure silt. All specimens prepared by air pluviation method showed higher *SSS* than that for specimens prepared by moist tamping method except clean sand.

The concept of equivalent granular void ratio was found to be more appropriate to explain the behaviour of sand-silt mixtures than the relative density and global void ratio.

In both moist tamping and air pluviation methods, the coefficient of permeability decreases with increasing nonplastic silt content till *LFC*; later it remains near about constant till the specimens become pure silt. This variation of coefficient of permeability with silt content was better explained by variation of effective particle size ( $D_{10}$ ) than relative density and void ratio.

## ACKNOWLEDGMENT

Financial support for this research work by Bangladesh University of Engineering and Technology is gratefully acknowledged.

## REFERENCE

- Arab, A., and Belkhatir, M. (2012). "Fines Content and Cyclic Preloading Effect on Liquefaction Potential of Silty Sand: A Laboratory Study." *Acta Polytechnica Hungarica* 9(4), 47-64.
- Belkhatir, M., Hanifi, M., Ahmed, A., Noureddine, D., and Tom, S. (2011). "Undrained Shear Strength of Sand-silt Mixture: Effect of Intergranular Void Ratio and Other Parameters." *KSCE Journal of Civil Engineering* (Springer) 15(8), 1335-1342.
- Belkhatir, M., Schanz, T., and Arab, A. (2013). "Effect of Fines Content and Void Ratio on the Saturated Hydraulic Conductivity and Undrained Shear Strength of Sand-silt Mixtures." *Environ Earth Sci* (Springer) 70(6), 2469-2479.
- Chang, N. Y., and Kaufman, L. P. (1982). "Liquefaction Potential of Clean and Silty Sands." Seattle, USA: Proceedings of the 3rd International Earthquake Microzonation, 1982. 1017-1032.
- Cetin, K. O., Seed, R. B., Kiureghian, A. D., Tokimatsu, K., Jr., L. F. H., Kayen, R. E., and Moss, R. E. S., (2014) "Standard Penetration Test-Based Probabilistic and Deterministic Assessment of Seismic Soil Liquefaction Potential." *Journal of Geotechnical and Geoenvironmental Engineering* (ASCE) 130(12): 1314-1340.
- Chu, J., and Leong, W. K., (2002) "Effect of Fines on Instability Behaviour of Loose Sand." *Geotechnique*, 52(10): 751-755.
- Dash, H K, and Sitharam, T. G. (2011a). "Undrained Monotonic Response of Sand-silt Mixtures: Effective of Nonplastic Fines." *Geomechanics and Geoenvironmental Engineering: An International Journal* (Taylor & Francis) 6(1), 47-58.
- Dash, H. K, and Sitharam, T. G. (2011b). "Undrained Cyclic and Monotonic Strength of Sand-Silt Mixtures." *Geotech Geol Eng* (Springer) 29(4), 555-570.
- Hazen, A. (1892) Some physical properties of sand and gravel, with special reference to their use in filtration. Massachusetts State Board of Health, Boston: 24th Annual Report.
- Hazirbaba, K. (2005). Pore pressure generation characteristics of sands and silty sands: a strain approach. Dissertation presented for PhD program to the faculty of Graduate School at the University of Texas at Austin.
- Karim, M. E. and Alam, M. J. (2014), "Effect of non-plastic silt content on the liquefaction behavior of sand-silt mixture." *Soil Dynamics and Earthquake Engineering*, 65, 142-150.
- Kresic, N. (1998) "Quantitative Solutions in Hydrogeology and Groundwater Modeling." Lewis Publishers.
- Lo, S. R., Rahman, M. M., and Bobei, D. C. (2008). "Limited flow behavior of sand with fines under monotonic and cyclic loading." *Geotechnical Engineering for Disaster Mitigation and Rehabilitation*, 201-209.
- Lee, K. L., and Fitton, J. A. (1968). "Factors affecting the cyclic loading strength of soil." *Vibration effects of earthquake on soils and foundation*, STP 450, ASTM, West Conshohocken, Pa., 71-95.
- Murthy, T. G., Loukidis, D., Carraro, J. A., Prezzi, M., and Salgado, R. (2007). "Undrained monotonic response of clean and silty sands." *Geotechnique*, 57(3) : 273-288.
- Pitman, T. D., Robertson, P. K., and Segoo, D. C., (1994). "Influence of Fines on the Collapse of Loose Sands." *Canadian Geotechnical Journal*, 31(5), 728-739.
- Rahman, M.M., and Lo, S.R. 2008. The prediction of equivalent granular steady state line of loose sand with fines. *Geomechanics and Geoenvironmental Engineering: An International Journal*, 3(3): 179-190. doi:10.1080/17486020802206867.
- Rahman, M. M., Lo, S. R., and Gnanendran, C. T., (2008) "On Equivalent Granular Void Ratio and Steady State Behaviour of Loose Sand with Fines." *Can. Geotech. J.* 45: 1439-1456
- Rahman, M. M., Baki, M. A. L., and Lo., S. R., (2014). "Prediction of Undrained Monotonic and Cyclic Liquefaction Behavior of Sand with Fines Based on the Equivalent Granular State Parameter." *International Journal of Geomechanics* (ASCE) 14, no. 2: 254-266.
- Rahman, M. M., Sik-Cheung Robert Lo, and Misko Cubrinovski. (2010), "On Equivalent Granular Void Ratio and Behaviour of Loose Sand." *Canadian Geotechnical Journal*, 45(10): 1439-1456.
- Rahman, M. M., Lo, S. R., and Baki, M. A. L. (2011). "Equivalent granular state parameter and undrained behaviour of sand-fines mixtures." *Acta Geotech.*, 6(4), 183-194.
- Seed, H. B., Idriss, I. M., and Arango, I. (1983). "Evaluation of Liquefaction Potential Using Field Performance Data." *Journal of Geotechnical Engineering* (ASCE) 109(3), 458-482.
- Sladen, J. A., D'Hollander, R. D., and Krahn, J., Mitchell, D. E. (1985). "Back Analysis of the Nerlerk Berm Liquefaction Slides." *Canadian Geotechnical Journal*, 22(4), 579-588.
- Thevanayagam, Sabanayagam. (2000) "Liquefaction Potential and Undrained Fragility of Silty Soils." 12WCEE 2000 Conference proceeding, New York, 1-8.

- Thevanayagam, S., Shenthan, T., and Liang, J., (2002). "Undrained Fragility of Clean Sands, Silty Sands, and Sandy Silt." *J. Geotech. Geoenviron. Eng.* 128: 849-859.
- Tokimatsu, K., and Yoshimi, Y. (1983). "Empirical Correlation of Soil Liquefaction Based on SPT N-Value and Fines Content." *Soils and Foundations* 23(4), 57-74.
- Troncoso, J. H., and Verdugo, R. (1985). "Silt Content and Dynamic Behavior of Tailing Sands." In *Proceedings of the 11th International Conference on Soil Mechanics and Foundation Engineering*. San Francisco, Calif., 1985. 1311-1314.
- Yamamoto, J. A., and Kelly, M. C. (2001). "Monotonic and Cyclic Liquefaction Of Very Loose Sands With High Silt Content." *Journal of Geotechnical and Geoenvironment Engineering* 127(4), 314-324.
- Yin, Z., Zhao, J., and Hicher, P. (2013). "A Micromechanics-Based Model for Sand-Silt Mixtures." *International Journal of Solids and Structures* (Elsevier) 51(6), 1350–1363.